International Conference on Applied Energy 2020
Dec. 1 - Dec. 10, 2020, Bangkok / Virtual
Paper ID: 232

Experimental study on flow and heat transfer characteristics of contact condensation in rectangular microchannels

Xiao LIU [1], Luanfang DUAN[2], Dongren LIU [1*]

1 School of mechanical engineering, Yangzhou University, Yangzhou, 225127, Jiangsu Province, China

2 School of Electrical Engineering, Nanjing Vocational university of industry Technology, Nanjing 210046, P. R. China

ABSTRACT

The flow and heat transfer characteristics of contact condensation in rectangular microchannels were studied experimentally. All tests were performed with water and steam. At a certain gas-liquid ratio, three flow patterns were found in the microchannel of 600 μm: slug flow, annular flow and mist flow. The experimental results show that the contact condensation heat transfer process in the microchannel is affected by the channel structure and gas-liquid flow. In the experimental conditions with higher Reynolds number, due to the influence of inertia force, the Nusselt number decreases with the increase of hydraulic diameter, and increases with the increase of flow rate. However, in the same microchannel, the Nu_x of the fluid reaches the maximum at the entrance, and then decreases gradually along the flow direction.

Keywords: Microchannel, Heat transfer, Condensation, Two-phase flow

NONMENCLATURE

Symbols	
H	depth of the channel
k	thermal conductivity
$\dot{m}$	total mass flow rate
Nu	Nusselt number
q	heat flux
Re	Reynolds number
T	temperature
Subscripts	
S	steam
L	liquid
x	X direction
w	wall

1. INTRODUCTION

Contact condensation is used widely in chemical industry, energy, aero-space and other fields. Such as micro-heat exchangers, cooling towers, electronic cooling systems in nuclear reactor, contact feed water heaters, water desalination units, etc. [1-4] Contact condensation can obtain higher heat transfer coefficient and higher heat transfer efficiency at a smaller temperature gradient.

Mahood [5] carried out an experimental study on the transient characteristics of the contact condenser with pentane steam and tap water as working fluids. The results showed that the liquid phase temperature increases with time, and the latent heat plays a dominant role in the direct contact condensation process. Xu [6] studied the condensation characteristics of direct contact condensation of stable steam jet in vertical pipe. The experimental results showed that the radial temperature decreases exponentially from the center of the pipe to the wall. The prediction model of average heat transfer coefficient and average Nusselt number related to steam mass flow and Reynolds number is proposed. An experimental study of condensation characteristics in rectangular microchannels by Mghari [7], the results showed that the condensation heat transfer coefficient increases with the increase of contact angle and decreases with the increase of hydraulic diameter.

The direct contact condensation process in a rectangular cross-section convective T-junction microchannel with adiabatic wall was studied by combining visualization method with heat transfer experiment. the flow and heat transfer characteristics of contact condensation process in rectangular cross-section microchannels with different hydraulic diameters were analyzed by using water and steam

Selection and peer-review under responsibility of the scientific committee of the 12th Int. Conf. on Applied Energy (ICAE2020).

instead of liquid nitrogen and VOCs gas, which laid the foundation for further study on the contact condensation method for VOCs recovery in microchannels.

2. MATERIAL AND METHODS

2.1 Experimental system

Fig. 1 shows the experimental system and flow diagram. The experimental system consists of steam generating system, microchannel test segment, visualization system and data acquisition system. Distilled water and saturated steam were used as the working fluid. The physical properties of the working fluid at standard atmospheric pressure are shown in Table 1.

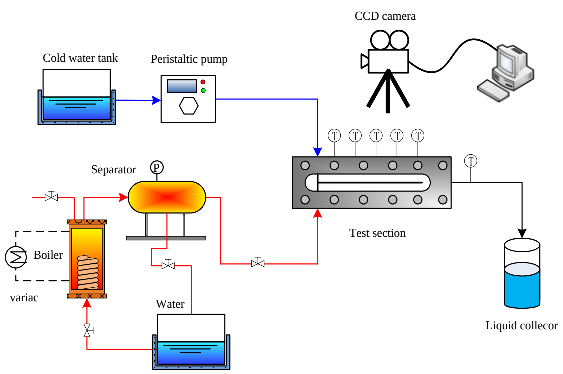

Fig 1 Schematic diagram of experimental setup.

Table.1Physical properties of the working fluids (1atm)

Fluid	Water	Steamr
Density (kg m^{-3})	997	0.58961
Viscosity (kg m^{-1}s^{-1})	9.78×10^{-4}	1.27×10^{-5}
Surface tension (N m^{-1})	0.072	—
Heat capacity (J kg^{-1} K^{-1})	4182	2080
Thermal conductivity (W m^{-1} K^{-1})	0.607	0.0242

2.2 Microchannel test segment

The structure and size of the microchannel test section are shown in Fig. 2. The width of the channel is 300 μm, and the depth is 300 μm, 600 μm and 900 μm, respectively. Symmetrical T-junction microchannel is used to realize gas-liquid two-phase contact heat transfer in the channel. The gas-liquid inlet is symmetrically distributed on both sides of the main channel, and an outlet is located at the bottom of the channel. five square channels with a diameter of 1.2mm are distributed under the center line of the main channel for install thermocouples. the top and main view of the thermocouple distribution is presented in Fig. 2.

3. DATA REDUCTION

In this paper, the processing of experimental data is based on the following assumptions:

(1) The influence of dissolved oxygen and other gases in water on heat transfer process is ignored.

(2) The change of total heat is equal to the change of fluid enthalpy value, so the energy conservation equation can be simply described by heat balance equation.

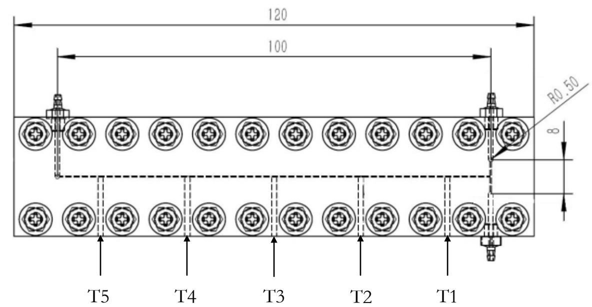

Fig 2 Diagram of thermocouple distribution.

In the experiment, the thermocouple is installed at the *H* point from the bottom of the channel. Therefore, the wall temperature T_w can be calculated by Fourier law:

$$T_w = T - \frac{q_w H_w}{k_w} \tag{1}$$

Where k_w, H_w and T are the thermal conductivity of 6063 aluminum alloy plate, wall thickness and the temperature collected by thermocouple data acquisition system, respectively.

The local mean fluid temperature T_{bi} (pseudo-local mean fluid temperature) can be calculated by heat balance:

$$\dot{m}\Delta H = \dot{m}c_p(T_{bi} - T_{bin}) = \sum_{j=1}^{i-1} Q_j + Q_i / 2 \tag{2}$$

The local Nusselt number Nu_x is calculated as follows:

$$Nu_x = \frac{q_w}{T_{wi} - T_{bi}} \times \frac{d}{k_L} \tag{3}$$

4. RESULTS AND DISCUSSION

4.1 Analysis of flow characteristics

When the steam flow rate is between 0.0022g/s and 0.0045g/s, there are three main flow patterns observed in the 600 μm microchannel: slug flow, annular flow and mist flow.

Fig. 3 is the condensation process of steam at G_S = 0.00375 g/s and G_L = 0.036 g/s. As the bubble moving downstream, the bubble length gradually decreases. the liquid column is in a completely closed microchannel, there is no liquid to supplement it directly. Therefore, we conclude that the increase of the length is due to the condensation of steam. the clear gas-liquid interface cannot be obtained in mist flow and annular flow, so the condensation mechanism of steam in these two flow patterns still needs to be further explored.

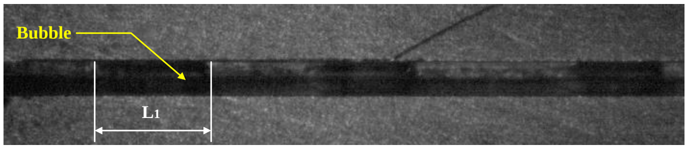

(a) t=0ms

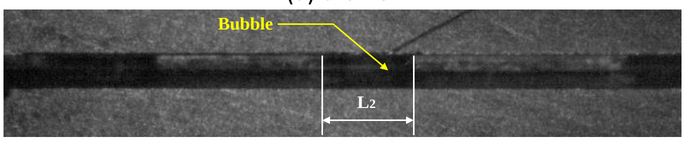

(b) t=0.6ms

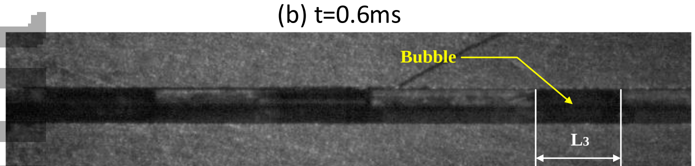

(c) t=1.2ms

Fig 3 Condensation process in microchannel.

4.2 Temperature distribution

Fig. 4 is the variation of wall temperature of microchannel with time at different depths under 300 m, 600 m and 900 m respectively under different operating conditions. Operating conditions are listed in table 2. In all experiments, the temperature of the inlet liquid was controlled at 11.2 ℃± 0.2 ℃. It can be seen from the figure that the change of temperature can be divided into two stages, the first stage is the rapid rise stage, the second stage is the nearly-stable stage.

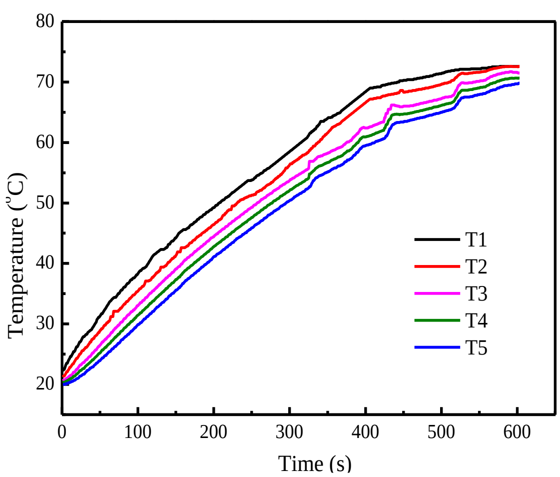

(a)H=900μm

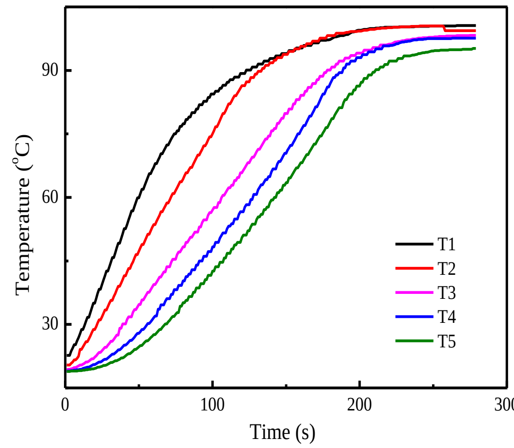

(b) H=600μm

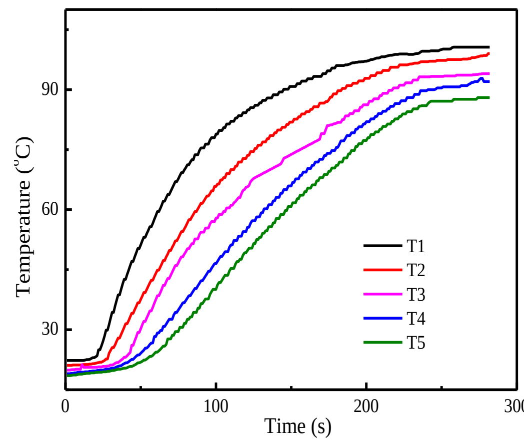

(c) H=300μm

Fig 4 Wall temperature distribution.

Fig. 5 is the distribution of temperature field along the flow direction of microchannel at different times. It can be seen from the figure that the wall temperature gradually decreases along the flow direction of the channel. It can also be seen from Fig. 5 that the temperature increases with time.

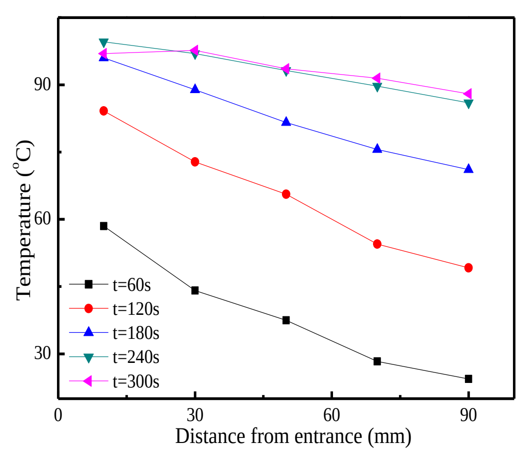

(a)H=300μm

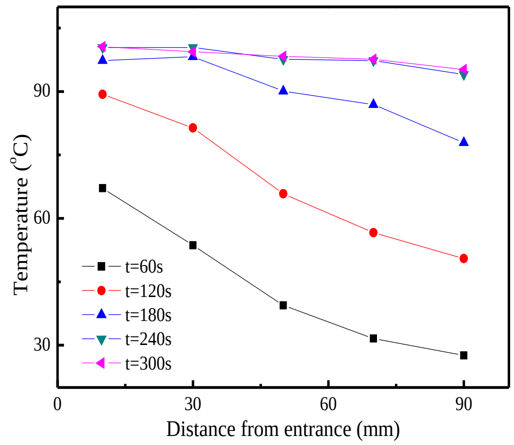

(b) H=600μm

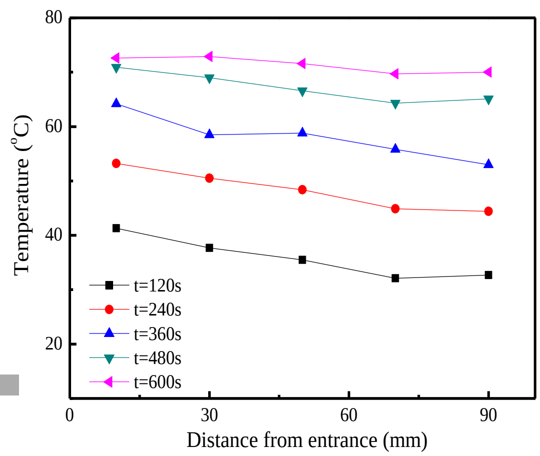

(c) H=900μm

Fig 5 Temperature distribution along flow direction.

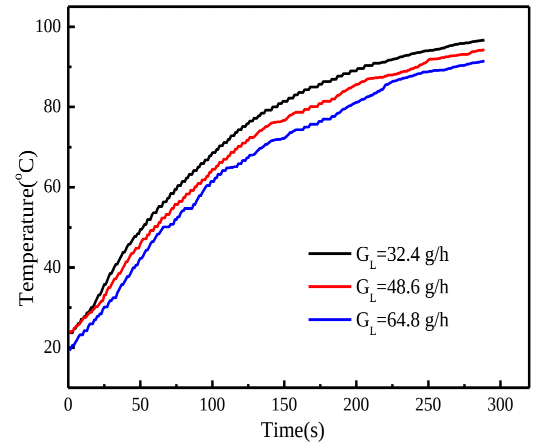

(a) H=600μm

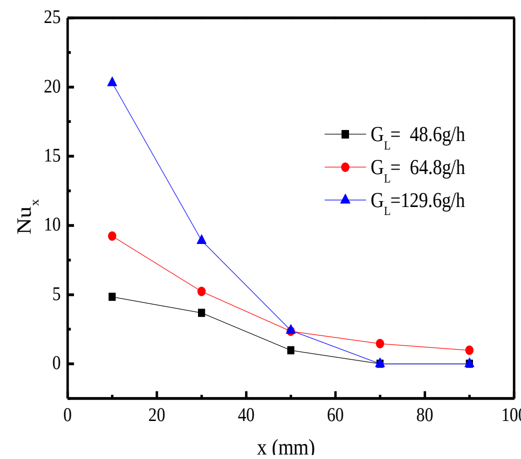

(b) H=600μm

Fig 6 Effect of mass flow rate.

4.3 Influence of flow rate

Fig. 6(a) is the change of temperature under different liquid flow rates measured in the microchannel with depth of 600 μm. As shown in Fig. 6(a), the wall temperature of microchannel increases with the increase of time under different liquid flow rates, and the rising speed is basically the same. However, at the same time point, the temperature of the channel wall decreases with the increase of liquid flow rate.

It can also be seen from Fig. 6(b) that the Nu_x of fluid heat transfer increases with the increase of flow rate. Because the Reynolds number *Re* of the fluid is high under the current experimental conditions, the heat transfer process is greater effect by the inertial force. The Nu_x of the fluid reaches the maximum at the entrance, and then decreases gradually along the flow direction.

4.4 Influence of channel diameter

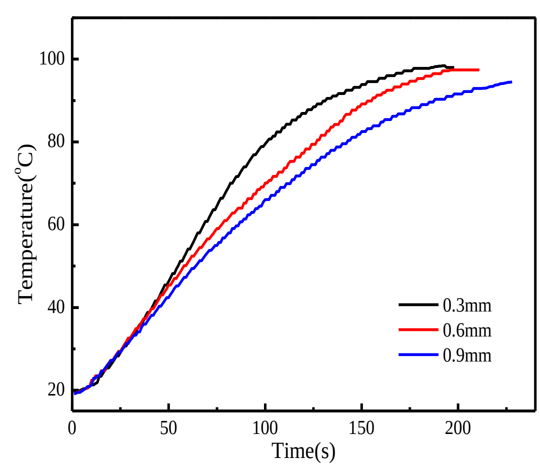

(a)

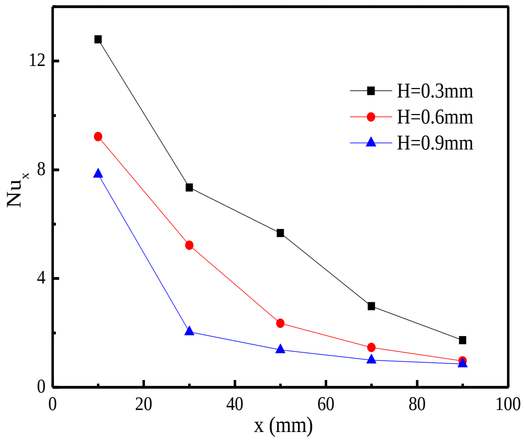

(b)

Fig 7 Effect of geometry size.

Fig. 7 is the change of temperature and Nu_x when the contact condensation is affected by the microchannel diameter. As shown in Fig. 7(a), when the liquid flow rate is constant at 129.6mL/h, the wall temperature of the channel increases with time, but the smaller the hydraulic diameter of the channel, the faster the temperature rise. At the same time point, the smaller the channel diameter, the higher the wall temperature. The results show that the hydraulic diameter of the channel has a great influence on the heat transfer under the same operating conditions. Fig. 7(b) is the change of local Nusselt number with hydraulic diameter. Nu_x increases gradually with the decrease of hydraulic diameter, which is due to the increase of fluid velocity and the decrease of effective heat transfer area in the channel under the condition of the constant other parameters. The decrease of effective heat transfer area makes the heat flux increase. According to the calculation formula of Nu_x, if the physical properties of the fluid remain unchanged, the increase of the heat flux will lead to the increase of Nu_x.

5. CONCLUSIONS

(1) Under the current experimental conditions, the flow pattern of contact condensation in microchannels is affected by gas-liquid ratio. With the increase of gas-liquid ratio, the flow pattern gradually changes from slug flow to annular flow, and finally to mist flow.

(2) The contact condensation heat transfer process in microchannels is mainly affected by channel structure and gas-liquid flow rate. The convective heat transfer coefficient decreases with the increase of hydraulic diameter and increases with the increase of flow rate. The reason is that the Reynolds number *Re* of the fluid is high under the current experimental conditions, and the heat transfer process is still greatly affected by the inertial force.

ACKNOWLEDGEMENT

The authors acknowledge the financial support provided by Natural Science Foundation of Jiangsu Province (No. BK20180936).

REFERENCE

[1] Chun M H, Kim Y, Park J, et al. An investigation of direct condensation of steam jet in subcooled water[J]. International Communications in Heat and Mass Transfer, 1996, 23(7): 947-958.
[2] Apanasevich P, Lucas D, Beyer M, et al. CFD based approach for modeling direct contact condensation heat transfer in two-phase turbulent stratified flows[J]. International Journal of Thermal ences, 2015, 95:123-135.
[3] Mghari H E, Asbik M, Louahliagualous H, et al. Condensation heat transfer enhancement in a horizontal non-circular microchannel[J]. Applied Thermal Engineering, 2014, 64(1): 358-370.
[4] Gulawani S S , Joshi J B , Shah M S , et al. CFD analysis of flow pattern and heat transfer in direct contact steam condensation[J]. Chemical Engineering Science, 2006, 61(16):5204-5220.
[5] Mahood H B, Thorpe R B, Campbell A N, et al. Experimental measurements and theoretical prediction for the transient characteristic of a two-phase two-component direct contact condenser[J]. Applied Thermal Engineering, 2015: 161-174
[6] Xu Q, Guo L, Zou S, et al. Experimental study on direct contact condensation of stable steam jet in water flow in a vertical pipe[J]. International Journal of Heat and Mass Transfer, 2013: 808-817.
[7] Mghari H E, Asbik M, Louahliagualous H, et al. Condensation heat transfer enhancement in a horizontal non-circular microchannel[J]. Applied Thermal Engineering, 2014, 64(1): 358-370.